

Rheological Study of Transient Networks with Junctions of Limited Multiplicity II. Sol/Gel Transition and Rheology

Tsutomu Indei*

*Fukui Institute for Fundamental Chemistry,
Kyoto University, Kyoto 606-8103, Japan*

Tel: +81-75-711-7894

Fax: +81-75-781-4757

Abstract

Viscoelastic and thermodynamic properties of transient gels formed by telechelic polymers are studied on the basis of the transient network theory that takes account of the correlation among polymer chains via network junctions. The global information of the gel is incorporated into the theory by introducing the elastically effective chains according to the criterion by Scanlan and Case. We also consider effects of superbridges whose backbone is formed by several chains connected in series with several breakable junctions inside. Near the critical concentration for the sol/gel transition, superbridges becomes infinitely long along the backbone, thereby leading to the short relaxation time τ of the network. It is shown that τ is proportional to the concentration deviation Δ near the gelation point. The plateau modulus G_∞ increases as the cube of Δ near the gelation point as a result of the mean-field treatment, and hence the zero-shear viscosity increases as $\eta_0 \sim G_\infty \tau \sim \Delta^4$. The dynamic shear moduli are well described in terms of the Maxwell model, and it is shown that the present model can explain the concentration dependence of the dynamic moduli for aqueous solutions of telechelic poly(ethylene oxide).

Keywords

associating polymers; transient network theory; junction multiplicity; sol/gel transition; Scanlan-Case criterion; superbridges;

*Electronic address: indei@fukui.kyoto-u.ac.jp

I. INTRODUCTION

Transient gels formed by associating polymers have been attracted widespread interests in recent years. [1] Associating polymers are polymer chains carrying specific groups capable of forming aggregates through noncovalent bonding.[2, 3, 4, 5, 6, 7, 8, 9, 10, 11] Above a certain polymer concentration, they form a transient gel by connecting sticky groups on polymers. This transformation is thermoreversible in general. In the previous paper[12] (referred to as I in the following), we presented a theoretical model of transient gels formed by junctions comprised of limited number of hydrophobic groups with an intention to understand thermodynamic properties of linear rheology of telechelic associating polymer systems. As the first attempt, elastically effective chains (or active chains) were defined locally, i.e., chains whose both ends are connected to other end groups are elastically effective irrespective of whether these groups are incorporated into an infinite network (gel) or not. We could explain, to some extent, the concentration dependence of the dynamic shear moduli described in terms of the Maxwell model, but the sol/gel transition of the system could not be treated properly due to the local definition of active chains.

In this paper, we take account of the global information of the infinite network by making use of the criterion suggested by Scanlan [13] and Case [14] for a chain to be active. This criterion states that telechelic chains are elastically effective if their both ends are connected to junctions with at least three paths to the infinite network. We assume that these chains deform according to the macroscopic deformations applied to the gel. Static properties of transient gels have been studied by Tanaka and Ishida on the basis of this criterion.[16] We here consider not only primary active chains (referred to as primary bridges in this paper) but also active superchains (called superbridges) whose backbone is an aggregate of several bridges connected in series. Effects of superbridges cannot be negligible especially when one study dynamical properties of transient gels because they enhance the relaxation time of the network due to a number of internal junctions possible to break as suggested by Annable *et al.*[2] We can describe the transition between the sol state and gel state (appearance of the infinite network) in this theoretical framework. The critical behavior of viscoelastic quantities near the sol/gel transition point is shown to be much affected by superbridges.

It has been established up to now that telechelic polymers self-assemble in dilute solution to form flowerlike micelles. Pham *et al.* [6, 7] indicated that the solution of flowerlike micelles resembles a colloidal dispersion of adhesive hard spheres in the concentration dependence of the shear modulus. Quite recently, Meng and Russel [11] showed that the colloidal theory describing the nonequilibrium structure of dispersions under shear explains the high-frequency plateau modulus of telechelic poly(ethylene oxide) (PEO). In this paper, we attempt to theoretically describe linear rheology of telechelic polymers in the absence of intramolecular associations. It can be shown that experimentally observed dynamic shear moduli that are characterized by the high-frequency plateau modulus, zero-shear viscosity and relaxation time, are well described in terms of this theoretical treatment. It indicates that the transient network theory is useful tool not only for the study of rheological but also for thermodynamic properties of transient gels when it is extended so that both the correlation among polymers and global structure of the network are taken into consideration.

This paper is organized as follows. In section II, we will review assumptions and definitions employed in I. They are also employed in this paper. In section III, linear viscoelasticities of the transient gel will be studied within the framework of the Scanlan-Case criterion for active chains. As the first step, only primary bridges are taken into consideration in this section. Effect of superbridges will be discussed in section IV. In section V, linear rheology including effects of superbridges will be studied. Section VI will be devoted to a summary.

II. ASSUMPTIONS AND DEFINITIONS OF FUNDAMENTAL QUANTITIES

We consider athermal solutions of n linear polymers (or primary chains) per unit volume. Functional groups capable of forming junctions through noncovalent bonding are locally embedded in both ends of the primary chain. Common assumptions employed in this paper and in I are as follows: 1) any number of functional groups are allowed to be bound together to form one junction; 2) reactions among functional groups are allowed to occur only in a stepwise manner; 3) primary chains are Gaussian chains; 4) the Rouse relaxation time of the primary chain is much smaller than the characteristic time of the macroscopic deformation applied to the system and the lifetime of association among functional groups; 5) the looped chain formed by a single primary chain is absent; 6) the molecular weight of the primary chain is much smaller than the entanglement molecular weight, and hence effects of the topological interaction among chains is ignored.

The terminology used in this paper (and I) are as follows: 1) the number of functional groups forming a junction (or the aggregation number), say k , is referred to as the junction multiplicity; 2) the junction with the multiplicity k is called the k -junction; 3) the primary chain whose head is incorporated into the k -junction whereas whose tail is a member of the k' -junction is referred to as the (k, k') -chain (we virtually mark one end of each chain to identify a

head and tail of the chain for convenience, although physical properties of the chain is homogenous along the chain); 4) the primary chain whose one end, irrespective of whether it is a head or tail, is incorporated into the k -junction is called the k -chain.

As in I, we define $F_{k,k'}(\mathbf{r}, t)d\mathbf{r}$ as the number of (k, k') -chains at time t per unit volume with the head-to-tail vector $\mathbf{r} \sim \mathbf{r} + d\mathbf{r}$. The total number of (k, k') -chains (per unit volume) is then given by

$$\nu_{k,k'}(t) = \int d\mathbf{r} F_{k,k'}(\mathbf{r}, t) = \nu_{k',k}(t) \quad (\text{II.1})$$

where two subscripts of $\nu_{k,k'}(t)$ are exchangeable due to the symmetry along the polymer chain. The total number of primary chains

$$n = \sum_{k \geq 1} \sum_{k' \geq 1} \nu_{k,k'}(t) \quad (\text{II.2})$$

is conserved independent of time. The number of k -chains is given by

$$\chi_k(t) = \sum_{k' \geq 1} \nu_{k,k'}(t), \quad (\text{II.3})$$

and then we can express the number of k -junctions as

$$\mu_k(t) = \frac{2\chi_k(t)}{k}. \quad (\text{II.4})$$

The number of functional groups belonging to k -junctions is $k\mu_k(t) = 2\chi_k(t)$ while the total number of functional groups is $2n$, so that the probability that an arbitrary chosen functional group is in a k -junction can be expressed as

$$q_k(t) = \frac{\chi_k(t)}{n}. \quad (\text{II.5})$$

Eq. (II.2) is equivalent to the normalization condition of q_k , i.e.,

$$\sum_{k \geq 1} q_k(t) = 1. \quad (\text{II.6})$$

The extent of reaction (or the probability for a functional group to be associated with other groups) is written as

$$\alpha(t) = \sum_{k \geq 2} q_k(t) = 1 - q_1(t). \quad (\text{II.7})$$

III. THEORY ON THE BASIS OF THE SCANLAN-CASE CRITERION FOR ACTIVE CHAINS

A. Global Structure of the Network

Here, we briefly review how to treat the global structure of the network according to refs. [16, 17, 18]. Above a certain concentration of primary chains, an infinite network (gel) is formed. In the postgel regime, the extent of reaction α' with regard to the functional groups in the sol part is different from that α'' in the gel part [18, 19]. Eq. (II.7) is the average extent of reaction for all functional groups in the system, i.e., it can be expressed as

$$\alpha(t) = \alpha'(t)w_S(t) + \alpha''(t)w_G(t) \quad (\text{III.1})$$

where $w_S(t)$ is the fraction of the sol part and $w_G(t) = 1 - w_S(t)$ is that of the gel. The sol fraction can be written as [16, 17, 18]

$$w_S(t) = \sum_{k \geq 1} q_k(t)\zeta_0^k, \quad (\text{III.2})$$

where ζ_0 is the probability that a randomly chosen unreacted group belongs to the sol part through its main chain. In the pregel regime, we have only $\zeta_0 = 1$. In the postgel regime, on the other hand, we have ζ_0 less than 1. Thus ζ_0

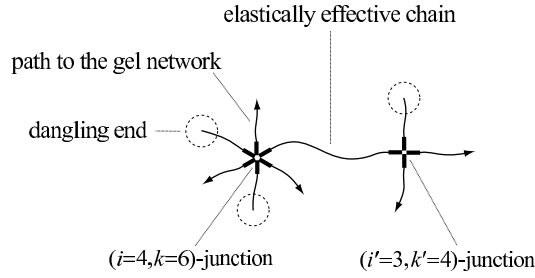


FIG. 1: The classification of the junction by the multiplicity k and the path connectivity i to the gel network. For example, a left-hand junction is formed by six functional groups but it is connected with the gel network only through four paths (represented by arrows); the other two paths are connected with dangling ends (indicated by dotted circles). A primary chain whose both ends are connected to the junctions with $i \geq 3$ is elastically effective.

is useful as an indicator of gelation. A primary chain belongs to the sol if its both ends are associated with the sol part, so that the sol fraction can be also expressed as

$$w_S(t) = \left(\sum_{k \geq 1} q_k(t) \zeta_0^{k-1} \right)^2. \quad (\text{III.3})$$

Therefore, ζ_0 is the root of the following equation

$$x = u(x), \quad (\text{III.4})$$

where

$$u(x) \equiv \sum_{k \geq 1} q_k(t) x^{k-1}. \quad (\text{III.5})$$

If (III.4) has more than one root, we must employ the smallest one.

Now we consider the connectivity of a functional group to the gel network according to the theoretical treatment by Pearson and Graessley [17]. Let $\mu_{i,k}$ be the number of junctions with multiplicity k that is connected to the gel network through i paths ($0 \leq i \leq k$). Such a junction is called the (i, k) -junction in the following. According to the multinomial theorem, it takes the form [16, 17]

$$\mu_{i,k}(t) = \mu_k(t) \frac{k!}{i!(k-i)!} \zeta_0^{k-i} (1 - \zeta_0)^i. \quad (\text{III.6})$$

Then the number of paths emerged from (i, k) -junction is $\chi_{i,k}(t) = (i/2)\mu_{i,k}(t)$. Here we employ the criterion of Scanlan [13] and Case [14] to decide whether the primary chain is active or not. They suggested that the primary chain whose both ends are connected to junctions with the path connectivity larger than or equal to 3 is elastically effective (see Fig.1). According to this criterion, the number of active chains whose one end is belonging to k -junctions is

$$\chi_k^{eff}(t) = \sum_{i \geq 3}^k \chi_{i,k}(t) = \chi_k(t) (1 - \zeta_0) [1 - \zeta_0^{k-1} - (k-1)\zeta_0^{k-2}(1 - \zeta_0)]. \quad (\text{III.7})$$

Note that $\chi_1^{eff}(t) = \chi_2^{eff}(t) = 0$. The total number of active chains is then given by [16]

$$\nu^{eff}(t) = \sum_{k \geq 3} \chi_k^{eff}(t) = n(1 - \zeta_0)^2 (1 - u'(\zeta_0)), \quad (\text{III.8})$$

where we have used a relation $\zeta_0 = u(\zeta_0)$. The number of active (k, k') -chains (i.e., the chain whose one end is connected to the (i, k) -junction with $i \geq 3$ and the other end is belonging to the (i', k') -junction with $i' \geq 3$) can be defined as

$$\nu_{k,k'}^{eff}(t) = \frac{\chi_k^{eff}(t) \chi_{k'}^{eff}(t)}{\nu^{eff}(t)}. \quad (\text{III.9})$$

The following relation

$$\sum_{k, k' \geq 3} \nu_{k,k'}^{eff}(t) = \nu^{eff}(t) \quad (\text{III.10})$$

holds as it should be.

B. Time-Development of Chains

The number of (k, k') -chains with the head-to-tail vector \mathbf{r} obeys the following time-evolution equation:

$$\frac{\partial F_{k,k'}(\mathbf{r}, t)}{\partial t} + \nabla \cdot (\dot{\mathbf{r}}_{k,k'}(\mathbf{r}, t) F_{k,k'}(\mathbf{r}, t)) = W_{k,k'}(\mathbf{r}, t) \quad (\text{for } k, k' \geq 3), \quad (\text{III.11})$$

where $\dot{\mathbf{r}}_{k,k'}(\mathbf{r}, t)$ is the rate of deformation of the head-to-tail vector \mathbf{r} of the (k, k') -chain. When a macroscopic deformation is applied to the gel, only active chains deform. Some (k, k') -chains are active but the other (k, k') -chains are not because each junction has the different path connectivity even if it has the same multiplicity. To take this into account, we put

$$\dot{\mathbf{r}}_{k,k'}(t) = P_{k,k'}(t) \hat{\kappa}(t) \mathbf{r} \quad (\text{III.12})$$

where $\hat{\kappa}(t)$ is the rate of deformation tensor applied to the gel, and

$$P_{k,k'}(t) \equiv \frac{\nu_{k,k'}^{eff}(t)}{\nu_{k,k'}(t)} \quad (\text{III.13})$$

is the probability for a (k, k') -chain to be active. Eq. (III.12) states that active chains deform affinely to the macroscopic deformation *on average*. Eq. (III.11) holds only for $k, k' \geq 3$ because both 1-junction and 2-junction cannot have path connectivity more than or equal to 3 and chains connected with such junctions do not deform. We assume that these elastically ineffective primary chains are Gaussian chains; i.e., the probability distribution function that they take the head-to-tail vector \mathbf{r} is

$$f_0(\mathbf{r}) \equiv \left(\frac{3}{2\pi N a^2} \right)^{3/2} \exp \left(-\frac{3|\mathbf{r}|^2}{2N a^2} \right) \quad (\text{III.14})$$

where N and a is the number and the length of the repeat unit constructing a primary chain, respectively. For example, the distribution function for the dangling chain is written as $F_{k,1}(\mathbf{r}, t) = \nu_{k,1}(t) f_0(\mathbf{r})$. The right-hand side of (III.11) represents the net increment of the (k, k') -chain per unit time due to the reaction between the end groups on the (k, k') -chain and the groups on the other chains. As shown in I, it takes the form

$$\begin{aligned} W_{k,k'}(\mathbf{r}, t) = & -[\beta_k(r) + \beta_{k'}(r) + B_k(t) + B_{k'}(t) + P_k(t) + P_{k'}(t)] F_{k,k'}(\mathbf{r}, t) \\ & + [p_{k-1}(t) \nu_{1,k'}(t) + p_{k'-1}(t) \nu_{k,1}(t)] f_0(\mathbf{r}) \\ & + B_{k+1}(t) F_{k+1,k'}(\mathbf{r}, t) + B_{k'+1}(t) F_{k,k'+1}(\mathbf{r}, t) \\ & + P_{k-1}(t) F_{k-1,k'}(\mathbf{r}, t) + P_{k'-1}(t) F_{k,k'-1}(\mathbf{r}, t) \quad (\text{for } k, k' \geq 3) \end{aligned} \quad (\text{III.15})$$

where $\beta_k(r)$ is the probability that a functional group is dissociated from the k -junction per unit time, and $p_k(t)$ is the probability for an unreacted group to be connected with the k -junction per unit time. As in I, we assume that the dissociation rate does not depend on the junction multiplicity nor the end-to-end length of the primary chain that is connected to the junction ($\beta_k(r) = \beta$). On the other hand, the connection rate p_k of the functional group with a k -junction is assumed to be proportional to the volume fraction of the k -junction, and we put $p_k(t) = \beta \lambda \psi q_k(t) h_k$ where $\lambda = \exp(\epsilon/k_B T)$ is the association constant (ϵ is the binding energy for the attraction of functional groups), $\psi = 2n\nu_0$ is the volume fraction of the functional group (ν_0 is the effective volume of a segment), and h_k is the factor depending on k that give a limitation on the junction multiplicity. In the following, we use $c \equiv \lambda \psi = 2\lambda\phi/N$ as a reduced polymer concentration ($\phi \equiv Nn\nu_0$ is the volume fraction of the primary chain). Under these assumptions, $B_k(t)$ and $P_k(t)$ in (III.15) are expressed as $B_k = \beta(k-1)$ and $P_k(t) = \beta k c q_1(t) h_k$, respectively.

The kinetic equation for (k, k') -chains has the same form as the one derived in I, i.e.,

$$\frac{d\nu_{k,k'}(t)}{dt} = w_{k,k'}(t) + w_{k',k}(t) \quad (\text{for } k, k' \geq 1), \quad (\text{III.16})$$

where

$$\begin{aligned} w_{k,k'}(t) = & -\beta k (1 + c q_1(t) h_k) \nu_{k,k'}(t) + \beta k \nu_{k+1,k'}(t) + (k-1) \beta c q_1(t) h_{k-1} \nu_{k-1,k'}(t) \\ & + \beta c h_{k-1} q_{k-1}(t) \nu_{1,k'}(t) \quad (\text{for } k \geq 2), \end{aligned} \quad (\text{III.17a})$$

$$w_{1,k'}(t) = \beta \left(\sum_{l \geq 2} \nu_{l,k'}(t) + \nu_{2,k'}(t) \right) - \beta c \left(\sum_{l \geq 1} h_l q_l(t) + h_1 q_1(t) \right) \nu_{1,k'}(t). \quad (\text{III.17b})$$

Note that (III.11) reduces to (III.16) by integrating it with respect to \mathbf{r} (for $k, k' \geq 3$). The kinetic equation for k -chains is obtained by taking a summation in (III.16) for overall k' . It takes the form

$$\frac{dq_k(t)}{dt} = \tilde{v}_k(t) \quad (\text{for } k \geq 1), \quad (\text{III.18})$$

where

$$\tilde{v}_k(t) = -\beta k(q_k(t) - q_{k+1}(t)) + \beta ck(h_{k-1}q_{k-1}(t) - h_k q_k(t))q_1(t) \quad (\text{for } k \geq 2), \quad (\text{III.19a})$$

$$\tilde{v}_1(t) = \beta \left(\sum_{l \geq 2} q_l(t) + q_2(t) \right) - \beta c \left(\sum_{l \geq 1} h_l q_l(t) + h_1 q_1(t) \right) q_1(t). \quad (\text{III.19b})$$

Once $q_k(t)$ is derived by solving (III.18), we can obtain the number of (k, k') -chains from the relation $\nu_{k,k'}(t) = nq_k(t)q_{k'}(t)$ and ζ_0 from (III.4), respectively. Then $\nu_{k,k'}^{eff}(t)$ and $P_{k,k'}(t) = \nu_{k,k'}^{eff}(t)/\nu_{k,k'}(t)$ can be obtained. By putting $P_{k,k'}(t)$ into (III.11) and solving the equations, we can derive $F_{k,k'}$.

We study two special models of junctions by putting a limitation on the multiplicity, i.e., the saturating junction model and the fixed multiplicity model [12, 15, 16]. In the saturating junction model, we allow junctions to take only a limited range of multiplicity $k = 1, 2, \dots, s_m$. This condition is realized by putting $h_k = 1$ for $1 \leq k \leq s_m - 1$ and $h_k = 0$ for $k \geq s_m$. If $s_m = \infty$, junction can take any value of multiplicity without limitation. In the fixed multiplicity model, all junctions can take only the same multiplicity s (except for $k = 1$). This situation can be approximately attained by introducing a small quantity $\delta (\ll 1)$ and by putting $h_k = \delta$ for $1 \leq k < s - 1$, $h_{s-1} = \delta^{-(s-2)}$, and $h_k = 0$ for $k > s - 1$. [12] We set $\delta = 0.01$ in most cases.

C. Equilibrium Properties

By putting $dq_k/dt = 0$ in (III.18), we can obtain q_k in equilibrium state. It turns out to be

$$q_k = \gamma_k c^{k-1} q_1^k \quad (\text{III.20})$$

where $\gamma_k = \prod_{l=1}^{k-1} h_l$ for $k \geq 2$ and $\gamma_1 = 1$. The fraction of unreacted groups q_1 is determined from the normalization condition $\gamma(z)q_1 = 1$, where $\gamma(z) \equiv \sum_{k \geq 1} \gamma_k z^{k-1}$ and $z \equiv cq_1$. The function defined by (III.5) can be expressed as $u(x) = \gamma(xz)/\gamma(z)$ in the equilibrium state, and hence ζ_0 is a solution of the following equation for a given z (or c):

$$x = \frac{\gamma(xz)}{\gamma(z)}. \quad (\text{III.21})$$

In the case that the junction can take any value of multiplicity without limitation, for example, z is smaller than 1 (see I) and hence $\gamma(z) = 1/(1-z)$ (we can put $h_k = 1$ for all k in this case). Thus ζ_0 is obtained as the smallest root of the equation $x = (1-z)/(1-xz)$, i.e.,

$$\zeta_0 = \begin{cases} 1 & (0 \leq z < z^*) \\ 1/z - 1 & (z^* < z \leq 1) \end{cases}, \quad (\text{III.22})$$

where $z^* = 1/2$. Note that z^* is interpreted as the critical value of the parameter z for the sol/gel transition. The number of elastically effective chain given by (III.8) is then analytically expressed as a function of z :

$$\nu^{eff} = \begin{cases} 0 & (0 \leq z < z^*) \\ n(2(z - z^*)/z)^3 & (z^* < z \leq 1) \end{cases}, \quad (\text{III.23})$$

We can also express these quantities as a function of c by the use of the relation $z = c/(1+c)$, that is,

$$\zeta_0 = \begin{cases} 1 & (c < c^*) \\ 1/c & (c > c^*) \end{cases}, \quad (\text{III.24})$$

and

$$\nu^{eff} = \begin{cases} 0 & (c < c^*) \\ n((c - c^*)/c)^3 & (c > c^*) \end{cases}, \quad (\text{III.25})$$

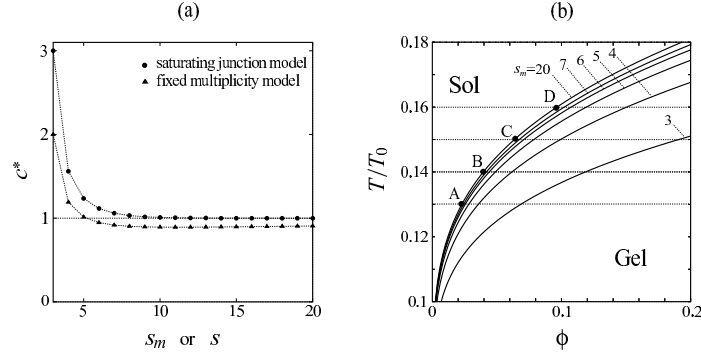


FIG. 2: (a) Reduced sol/gel transition concentration for the saturating junction model (circles) plotted against the maximum multiplicity s_m and for fixed multiplicity model (triangles) plotted against the multiplicity s . (b) Sol/gel transition curves drawn in the temperature-volume fraction plane for saturating junction model with $\lambda_0 = 1$ and $N = 100$. The maximum multiplicity is varying from curve to curve. See also Fig.9.

where $c^* = 1$ is the critical reduced concentration for gelation (see Fig.2 (a) for the case of limited multiplicity). Near the sol/gel transition point, the number of elastically effective chains increases as the cube of the concentration deviation,[16] i.e., $\nu^{eff} \simeq \Delta^3$ where $\Delta \equiv (c - c^*)/c^*$. In the high concentration limit, on the other hand, all primary chains become elastically effective, i.e., $\nu^{eff} \rightarrow n$ for $c \rightarrow \infty$.

In general, the sol/gel transition point is obtained as the point at which ζ_0 becomes lower than 1. This is equivalent to the point where the weight-average molecular weight of the cluster diverges. For polycondensation by multiple reaction, Fukui and Yamabe have shown that this condition (an appearance of the macroscopic cluster) is given by[23]

$$(f_w - 1)(\mu_w - 1) = 1 \quad (\text{III.26})$$

where $f_w (=2$ for the present model) is the weight-average functionality of the primary chain, and μ_w is the weight-average multiplicity of the junctions given by

$$\mu_w \equiv \sum_{k \geq 1} k q_k = 1 + \frac{z\gamma'(z)}{\gamma(z)}. \quad (\text{III.27})$$

A boundary curve separating the sol region and gel region in the temperature-concentration plane can be drawn by the use of the equation $2\lambda(T^*)\phi^*/N = c^*$ where T^* and ϕ^* are the critical temperature and volume fraction of the primary chain, respectively, and c^* is obtained according to the procedure stated above. Since the binding free energy is comprised of the energy part ϵ_0 and the entropy part S_0 , the association constant is rewritten as $\lambda(T) = \lambda_0 \exp(T_0/T)$ with $\lambda_0 \equiv \exp(-S_0/k_B)$ and $T_0 \equiv \epsilon_0/k_B$. Thus we have

$$T^* = T_0 / \log(Nc^*/2\lambda_0\phi^*). \quad (\text{III.28})$$

Fig.2 (b) shows the sol/gel boundary lines given by (III.28) for the saturating junction model as an example.

D. Dynamic-Mechanical and Viscoelastic Properties

We now apply a small oscillatory shear deformation with an amplitude ϵ to the gel network. A xy component of the rate of this deformation tensor is represented by $\kappa_{xy}(t) = \epsilon\omega \cos \omega t$ while the other components are 0 (ω is the frequency of the oscillation). Let us expand $F_{k,k'}(\mathbf{r}, t)$ with respect to the powers of ϵ up to the first order:

$$F_{k,k'}(\mathbf{r}, t) = F_{k,k'}^{(0)}(\mathbf{r}) + \epsilon F_{k,k'}^{(1)}(\mathbf{r}, t). \quad (\text{III.29})$$

We can put (see I)

$$F_{k,k'}^{(0)}(\mathbf{r}) = \nu_{k,k'} f_0(\mathbf{r}), \quad (\text{III.30a})$$

$$F_{k,k'}^{(1)}(\mathbf{r}, t) = \left(g'_{k,k'}(\omega) \sin \omega t + g''_{k,k'}(\omega) \cos \omega t \right) \frac{3xy}{Na^2} f_0(\mathbf{r}). \quad (\text{III.30b})$$

The number of (k, k') -chains does not depend on time as far as the small shear deformation is concerned,[20, 21, 22] so that $\nu_{k,k'}(t)$ and $q_k(t)$ can be represented by their equilibrium values $\nu_{k,k'}$ and q_k given above, respectively. Then the probability for a (k, k') -chain to be elastically effective is given by its equilibrium value $P_{k,k'} = \nu_{k,k'}^{eff} / \nu_{k,k'}$ with

$$\nu_{k,k'}^{eff} = \nu_{k,k'} \frac{[1 - \zeta_0^{k-1} - (k-1)\zeta_0^{k-2}(1 - \zeta_0)] [1 - \zeta_0^{k'-1} - (k'-1)\zeta_0^{k'-2}(1 - \zeta_0)]}{1 - z\gamma'(\zeta_0 z) / \gamma(z)}. \quad (\text{III.31})$$

The in-phase $g'_{k,k'}(\omega)$ and out-of-phase $g''_{k,k'}(\omega)$ amplitude of $F_{k,k'}^{(1)}$ are directly related with the storage and loss modulus of (k, k') -chains through the relations $G'_{k,k'}(\omega) = k_B T g'_{k,k'}(\omega)$ and $G''_{k,k'}(\omega) = k_B T g''_{k,k'}(\omega)$, respectively. Since primary chains are symmetric along the chain, two subscripts are exchangeable, i.e., $g'_{k,k'} = g'_{k',k}$ (and $g''_{k,k'} = g''_{k',k}$). Note that $g'_{k,1} = g''_{k,1} = g'_{k,2} = g''_{k,2} = 0$ for $k \geq 1$ since 2-chains and 1-chains are effectively in equilibrium state. By substituting (III.29) with (III.30) into (III.11), we have a set of equations for $g'_{k,k'}$ and $g''_{k,k'}$ as follows

$$g'_{k,k'} = (-Q_{k,k'} g''_{k,k'} + B_{k+1} g''_{k+1,k'} + B_{k'+1} g''_{k',k'+1} + P_{k-1} g'_{k-1,k'} + P_{k'-1} g'_{k',k'-1}) / \omega + \nu_{k,k'}^{eff}, \quad (\text{III.32a})$$

$$g''_{k,k'} = (Q_{k,k'} g'_{k,k'} - B_{k+1} g'_{k+1,k'} - B_{k'+1} g'_{k',k'+1} - P_{k-1} g'_{k-1,k'} - P_{k'-1} g'_{k',k'-1}) / \omega \quad (\text{for } k, k' \geq 3) \quad (\text{III.32b})$$

where $B_k = \beta(k-1)$, $P_k = \beta k c q_1 h_k$, $Q_{k,k'}(t) \equiv \beta k(1 + c q_1 h_k) + \beta k'(1 + c q_1 h_{k'})$, and $\nu_{k,k'}^{eff}$ is given by (III.31). It should be emphasized here that the last term in the right-hand side of (III.32a) is $\nu_{k,k'}^{eff}$ instead of $\nu_{k,k'}$ (see I as a reference). This is a consequence of the assumption (III.12).

The total moduli within the framework of the Scanlan-Case criterion for elastically effective chains are given by taking a summation of $G'_{k,k'}(\omega)$ and $G''_{k,k'}(\omega)$ over $k, k' \geq 3$, i.e.,

$$G'(\omega) = k_B T \sum_{k \geq 3} \sum_{k' \geq 3} g'_{k,k'}(\omega), \quad (\text{III.33a})$$

$$G''(\omega) = k_B T \sum_{k \geq 3} \sum_{k' \geq 3} g''_{k,k'}(\omega). \quad (\text{III.33b})$$

They are well described in terms of the Maxwell model with a single relaxation time (not shown here). In the high frequency limit, (III.32a) becomes $g'_{k,k'}(\omega \rightarrow \infty) = \nu_{k,k'}^{eff}$. Therefore, the plateau modulus defined by $G_\infty \equiv G'(\omega \rightarrow \infty)$ can be expressed as

$$G_\infty = \nu^{eff} k_B T = n k_B T (1 - \zeta_0)^2 \left(1 - \frac{z\gamma'(\zeta_0 z)}{\gamma(z)} \right). \quad (\text{III.34})$$

The reduced plateau modulus $G_\infty / (n k_B T)$ coincides with the number of active chains derived by Tanaka and Ishida for telechelic polymers.[16] As they have shown, it agrees well with experimental data for aqueous solution of hydrophobically modified ethylene oxide-urethane copolymers (called HEUR) reported by Annable *et al.*[2] On the other hand, the relaxation time τ of the gel determined from the peak position of (III.33b) does not agree well with experiments as in the case of I because it depends on c only weakly. This discrepancy can be ascribed to the absence of *superbridges* in elastically effective chains. A superbridge is a linear cluster of primary chains whose backbone includes a number of junctions with the path connectivity $i = 2$ to the gel network. Both ends of a superbridge are connected to junctions with the path connectivity $i \geq 3$. Fig.3 shows an example of the superbridge whose backbone is formed by four primary chains. In the Scanlan-Case criterion, superbridges are not regarded as the elastically effective chains; only *primary bridges*, or active primary chains (see Fig.3), are assumed to be responsible for the elasticity of the network. If we take superbridges into account, not only that the number of active chains becomes larger, but that the relaxation time of the network becomes shorter since their lifetime is shorter than that of primary bridge due to breakable node inside the backbone. We will discuss the effects of superbridges on $G'(\omega)$ and $G''(\omega)$ in the next section.^a

^a We use the nomenclature superbridge after ref.[2] where a cluster formed by connecting flower micelles linearly through bridges is called the superbridge. Their effects on the relaxation time is roughly estimated in this reference. In this paper, we count the number of superbridges in more detailed way by making use of the path connectivity to study their effect on the relaxation time.

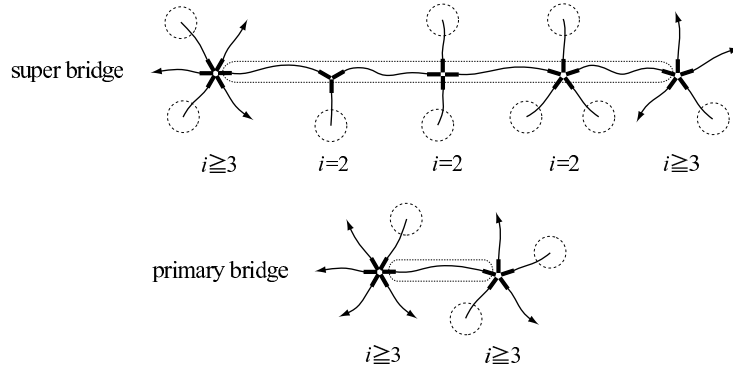


FIG. 3: Upper: schematic representation of a superbridge (surrounded by dotted ellipsoid). Lower: schematic representation of a primary bridge (or active primary chain).

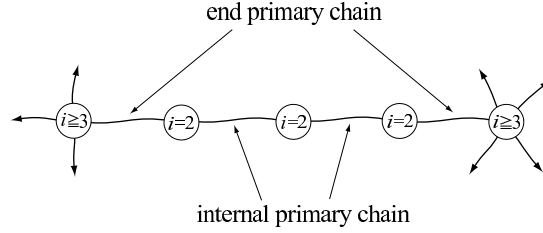


FIG. 4: A schematic of a superbridge (only paths to the network are drawn). It is comprised of two end primary chains and several internal primary chains. The number of end primary chains is written as $m(i \geq 3, i' = 2)$ whereas the number of internal primary chains is $m(i = 2, i' = 2)$.

IV. EFFECTS OF SUPERBRIDGES

A. Number of Superbridges

Let $m(i, i')$ be the number of primary chains whose one end is connected to the junction with the path connectivity i to the gel whereas the other end is connected to the junction with the connectivity i' . The number of primary bridges is then represented as^b

$$m(i \geq 3, i' \geq 3) = n(1 - \zeta_0)^2 \left(1 - \frac{z\gamma'(\zeta_0 z)}{\gamma(z)} \right) \equiv \nu_{SC}^{eff}. \quad (\text{IV.1})$$

The total number of primary chains incorporated into the gel through both ends is

$$m(i \geq 2, i' \geq 2) = \sum_{k \geq 2} \sum_{i \geq 2} \chi_{i,k} = n(1 - \zeta_0)^2 \equiv \tilde{\nu}^{eff}, \quad (\text{IV.2})$$

and the number of primary chains comprising backbones of superbridges is

$$m(i \geq 2, i' = 2) = \sum_{k \geq 2} \chi_{2,k} = n(1 - \zeta_0)^2 \frac{z\gamma'(\zeta_0 z)}{\gamma(z)} \equiv \nu_{pseud}^{eff}. \quad (\text{IV.3})$$

A relation $\tilde{\nu}^{eff} = \nu_{SC}^{eff} + \nu_{pseud}^{eff}$ holds as it should be. Near the sol/gel transition concentration (or $\Delta = (c - c^*)/c^* \ll 1$), these quantities increase as $\nu_{pseud}^{eff} \sim \tilde{\nu}^{eff} \sim \Delta^2$ (and $\nu_{SC}^{eff} \sim \Delta^3$) because $1 - \zeta_0$ is proportional to Δ while $z\gamma'(\zeta_0 z)/\gamma(z)$ is proportional to c . Since the superbridge is comprised of two end primary chains and a number of internal primary

^b We denote the number of primary bridge as ν_{SC}^{eff} instead of ν^{eff} in the rest of this article.

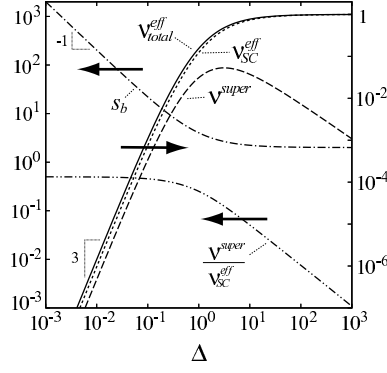


FIG. 5: The total number of elastically effective chain (solid line), the number of primary bridges or elastically effective chains defined on the basis of the Scanlan-Case criterion (dotted line), the number of super bridge (broken line), the number of primary chains per a super bridge (dash-dotted line), the ratio between the number of superbridges and the number of primary bridges (dash-double dotted line) plotted against relative concentration deviation $\Delta = (c - c^*)/c^*$ for the saturating junction model with the maximum multiplicity fixed at $s_m = 15$.

chains (see Fig.4), we have a relation $\nu_{pseud}^{eff} = m(i = 2, i' = 2) + m(i \geq 3, i' = 2)$ where

$$m(i = 2, i' = 2) = \sum_{k \geq 2} \sum_{k' \geq 2} \tilde{\nu}^{eff} \frac{\chi_{2,k}}{\tilde{\nu}^{eff}} \frac{\chi_{2,k'}}{\tilde{\nu}^{eff}} = \frac{(\nu_{pseud}^{eff})^2}{\tilde{\nu}^{eff}} \quad (IV.4)$$

is the number of internal primary chains, and

$$m(i \geq 3, i' = 2) = \nu_{pseud}^{eff} - m(i = 2, i' = 2) = \frac{\nu_{SC}^{eff} \cdot \nu_{pseud}^{eff}}{\tilde{\nu}^{eff}} \quad (IV.5)$$

is the number of end primary chains. In (IV.4), $\chi_{2,k}/\tilde{\nu}^{eff}$ is the probability for a chain in the network to be connected with the $(i = 2, k)$ -junction, and hence $\tilde{\nu}^{eff} (\chi_{2,k}/\tilde{\nu}^{eff}) (\chi_{2,k'}/\tilde{\nu}^{eff})$ is the number of primary chains whose one end is connected with the $(i = 2, k)$ -junction while the other end is belonging to the $(i' = 2, k')$ -junction. The number of superbridges is a half of the number of end primary chains of superbridges, i.e.,

$$\nu^{super} = \frac{1}{2} m(i \geq 3, i' = 2) = \frac{\nu_{SC}^{eff} \cdot \nu_{pseud}^{eff}}{2\tilde{\nu}^{eff}}. \quad (IV.6)$$

Therefore, the total number of elastically effective chain is turned out to be

$$\begin{aligned} \nu_{total}^{eff} &= \nu_{SC}^{eff} + \nu^{super} \\ &= n(1 - \zeta_0)^2 \left(1 - \frac{z\gamma'(\zeta_0 z)}{\gamma(z)} \right) \left(1 + \frac{z\gamma'(\zeta_0 z)}{2\gamma(z)} \right). \end{aligned} \quad (IV.7)$$

Fig.5 shows ν_{total}^{eff} together with the number ν_{SC}^{eff} of primary bridges, the number ν^{super} of superbridges, and the relative amount of the superbridges $\nu^{super}/\nu_{SC}^{eff}$ compared with primary bridges as a function of Δ for the saturating junction model ($s_m = 15$). The number of superbridges increases ($\nu^{super} \sim \Delta^3$) near the sol/gel transition concentration, but it decreases at higher concentration since the number of dangling ends decreases. Thus a peak appears in ν^{super} at a modest concentration. It should be emphasized that $\nu^{super}/\nu_{SC}^{eff}$ increases with decreasing Δ , and it finally reaches 0.5 for $\Delta \rightarrow 0$ although both ν^{super} and ν_{SC}^{eff} become close to 0 in this limit. It indicates that the effect of superbridges cannot be ignored as compared with primary bridges especially in the vicinity of the sol/gel transition point. Fig.5 also show the number of primary chains forming a superbridge given by

$$s_b \equiv \frac{\nu_{pseud}^{eff}}{\nu^{super}}. \quad (IV.8)$$

With decreasing Δ , many primary chains become incorporated into superbridges as $s_b \sim 1/\Delta$ (for $\Delta \ll 1$) indicating that the superbridge becomes longer along the backbone. With increasing concentration, on the contrary, s_b approaches to 2 since $m(i = 2, i' = 2)$ becomes close to 0. Summarizing, in the vicinity of the sol/gel transition concentration, (i) the superbridge is comparable in number to the primary bridge although both are few, and (ii) the superbridge is infinitely long.

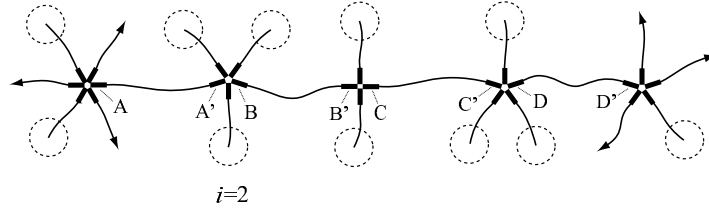


FIG. 6: An example of the superbridge whose backbone is comprised of $s_b(=4)$ primary chains.

B. Breakage Rate of Superbridge

Let us here focus on a primary chain whose one end is connected to the junction (say A) with the path connectivity $i_A \geq 3$ while the other end is belonging to the junction (A') with the path connectivity $i_{A'} \geq 2$. Such a primary chain is elastically effective.^c If $i_{A'} \geq 3$, then the chain is a primary bridge, so that the dissociation rate of the end group from the junction A' is β . If $i_{A'} = 2$, on the other hand, the chain is the end primary chain of the superbridge (see Fig.6), and we assume that the breakage rate of internal chains from the junctions B, B', C, ... is reflected in the dissociation rate of this end primary chain from the junction A'. Then we can put it as the sum of its own dissociation rate β and the dissociation rate $2(s_b - 1)\beta$ of $2(s_b - 1)$ functional groups B, B', ... on the internal primary chains. As a result, the dissociation rate of A' on average can be expressed as $\beta + 2(s_b - 1)\rho\beta \equiv \beta^{eff}$, where ρ is the probability for $i_{A'}$ to be 2 and is given by $\rho = m(i \geq 3, i' = 2) / (m(i \geq 3, i' \geq 3) + m(i \geq 3, i' = 2)) = \nu_{pseud}^{eff} / (\tilde{\nu}^{eff} + \nu_{pseud}^{eff})$. We replace β in (III.32) with β^{eff} in the following in order to incorporate the short lifetime of superbridges into account. It should be noted that the equilibrium condition (III.20) still holds after this replacement, so that the discussion given in III C and IV A of this paper and IV in I remains valid. When Δ is small, β^{eff} is inversely proportional to Δ since $s_b \sim 1/\Delta$ while $\rho \sim 1$ for $\Delta \ll 1$. Therefore, we see that the relaxation time τ of the gel that is approximately given as the reciprocal of β^{eff} is proportional to Δ near the sol/gel transition concentration.

Let $\tilde{P}_{k,k'}^{total}$ be the probability for a (k, k') -chain to be a primary bridge or an end primary chain of a superbridge. It is given by

$$P_{k,k'}^{total} = \frac{(\nu_{total}^{eff})_{k,k'}}{\nu_{k,k'}}, \quad (IV.9)$$

where

$$(\nu_{total}^{eff})_{k,k'} = \frac{\nu_{total}^{eff}}{2} \left(\frac{\chi_k^{eff} \tilde{\chi}_{k'}^{eff}}{\nu_{SC}^{eff} \tilde{\nu}^{eff}} + \frac{\tilde{\chi}_k^{eff} \chi_{k'}^{eff}}{\tilde{\nu}^{eff} \nu_{SC}^{eff}} \right) \quad (IV.10)$$

is the number of (k, k') -chains that is the primary bridge or the end primary chain of the superbridge. ($\tilde{\chi}_k^{eff} \equiv \sum_{i=2}^k \chi_{i,k} = \chi_k(1 - \zeta_0)(1 - \zeta_0^{k-1})$ is the number of paths (≥ 2) emerged from the $k(\geq 2)$ -junction, and hence $\tilde{\chi}_k^{eff} / \tilde{\nu}^{eff}$ is the probability that a k -junction satisfies the condition $i \geq 2$. On the other hand, $\chi_k^{eff} / \nu_{SC}^{eff}$ is the probability for a k -junction to fulfill the condition $i \geq 3$. Eq. (IV.10) is expressed in a symmetric form.) Eq. (IV.10) satisfies the following relation:

$$\sum_{k \geq 2} \sum_{k' \geq 2} (\nu_{total}^{eff})_{k,k'} = \nu_{total}^{eff} \quad (IV.11)$$

as it should be.^d If a macroscopic deformation is applied to the gel, not only primary bridges but also superbridges deform accordingly. According to (III.12), we assume that the rate of deformation vector of the (k, k') -chain is given

^c Internal primary chains of the superbridge (i.e., chains whose both ends are connected to the junctions with the path connectivity two) are also elastically effective in a sense that they are ingredients of the superbridge. However, these chains can be treated in this theoretical framework only indirectly as in the previous theory.[2] Effects of these internal chains are taken into account via the end primary chains of the superbridge in the rest of this paper. For example, the breakage rate of internal chains is reflected in the dissociation rate of the end primary chains. Furthermore, the elasticity of superbridges is represented by that of the end primary chains by assuming that the end primary chains deform affinely (see (IV.12)). This is valid when the macroscopic deformation applied to the gel is small as in the present case.

^d Note that $\chi_2^{eff} / \nu_{SC}^{eff} = 0$.

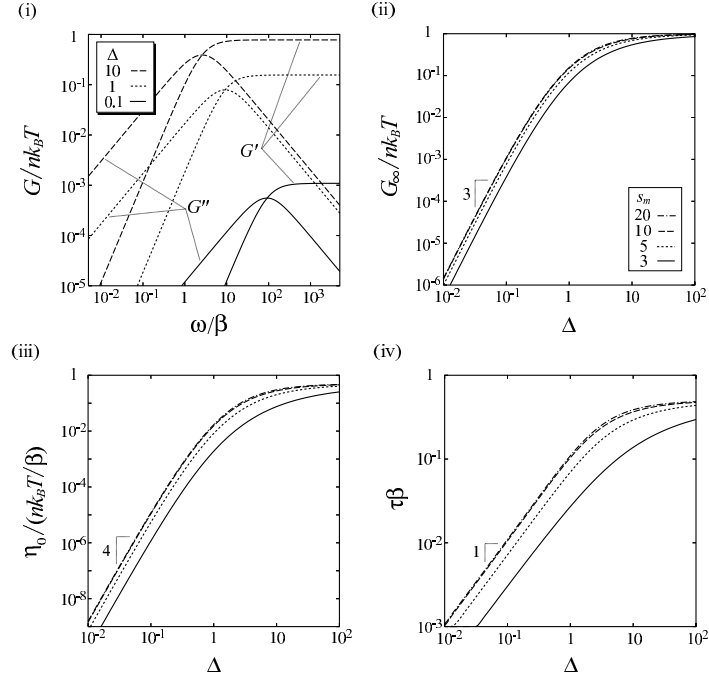


FIG. 7: (i) The dynamic shear moduli (reduced by $nk_B T$) for the saturating junction model as a function of the frequency. The relative concentration deviation $\Delta = (c - c^*)/c^*$ from the sol/gel transition concentration c^* is varying from curve to curve, while the maximum multiplicity of the junction is fixed at $s_m = 20$. (ii) The reduced plateau modulus, (iii) reduced zero-shear viscosity, and (iv) relaxation time plotted against the relative concentration deviation for several maximum multiplicities (increasing from bottom to top).

by

$$\dot{\mathbf{r}}_{k,k'}(t) = \tilde{P}_{k,k'}^{total} \hat{\kappa}(t) \mathbf{r}. \quad (\text{IV.12})$$

By substituting (IV.12) into (III.11), we can obtain the equations for $g_{k,k'}^{(n)}$ that is given by (III.32) but with $(\nu_{total}^{eff})_{k,k'}$ instead of $\nu_{k,k'}^{eff}$. Therefore, in the high frequency limit, $g_{k,k'}'$ reduces to $(\nu_{total}^{eff})_{k,k'}$. The total (observable) modulus is given by

$$G^{(n)}(\omega) = k_B T \sum_{k \geq 2} \sum_{k' \geq 2} g_{k,k'}^{(n)}(\omega), \quad (\text{IV.13})$$

and then we find $G' \rightarrow G_\infty = k_B T \nu_{total}^{eff}$ for $\omega \rightarrow \infty$.

V. RESULTS AND DISCUSSIONS

A. Saturating Junction Model

Fig.7 (i) shows the dynamic shear moduli calculated from (IV.13) for the saturating junction model. Relative concentration deviation is varying from curve to curve. They are well described in terms of the Maxwell model with a single relaxation time. Near the sol/gel transition concentration ($\Delta \ll 1$), the plateau modulus and the relaxation time increase as $G_\infty \sim \Delta^3$ (see Fig.7 (ii)) and $\tau \sim \Delta$ (Fig.7 (iv)), respectively. As a result, the zero shear viscosity increases as $\eta_0 \sim G_\infty \tau \sim \Delta^4$ (Fig.7 (iii)). Note that these powers stem from the mean-field treatment.^e For example, we can explain $\tau \sim \Delta$ as follows. Let ξ be the radius of gyration of the superbridge. If we assume that the superbridge

^e Rubinstein and Semenov have found the same power laws from the mean-field treatment for multifunctional polymers that can connect with each other through pairwise association between functional groups on polymers.[24]

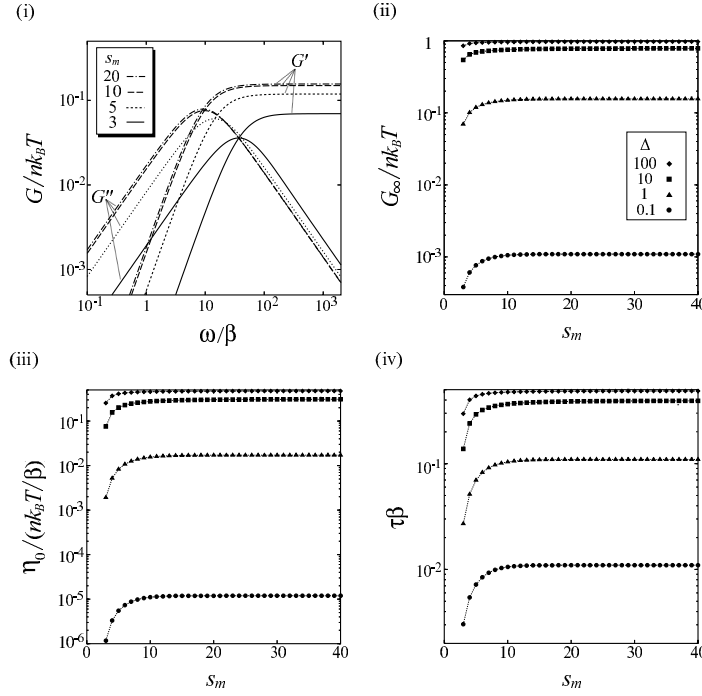


FIG. 8: (i) The dynamic shear moduli (reduced by $nk_B T$) obtained for the saturating junction model as a function of the frequency. The maximum multiplicity s_m is varying from curve to curve with a relative concentration deviation fixed at $\Delta = 1$. (ii) The reduced plateau modulus, (iii) reduced zero-shear viscosity, and (iv) relaxation time plotted against the maximum multiplicity for several relative concentration deviation (increasing from bottom to top).

obeys the Gaussian statistics, it is estimated to be $\xi \sim s_b^{1/2}$. On the other hand, ξ corresponds to the network mesh size, and hence it obeys the scaling law $\xi \sim \Delta^{-\nu}$ with $\nu = 1/2$ for $\Delta \ll 1$. By comparing two expressions, we can find $s_b \sim 1/\Delta$. Thus the mean lifetime of bridges (primary bridges and superbridges) that corresponds to the relaxation time of the network is approximately estimated to be $\tau \sim 1/[\beta + 2(s_b - 1)\rho\beta] \sim \Delta/\beta$. Fig.8 shows the dynamic shear moduli as a function of the maximum multiplicity s_m . The relaxation time increases with s_m because the number of superbridges decreases as s_m increases.

The reduced plateau modulus explicitly depends only on the reduced polymer concentration and the maximum multiplicity of the junction. Therefore, it is written as

$$\frac{G_\infty}{nk_B T} = f_1(c, s_m). \quad (\text{V.1})$$

Similarly, the reduced zero-shear viscosity and the relaxation time can be expressed as

$$\frac{\beta\eta_0}{nk_B T} = f_2(c, s_m) \quad (\text{V.2})$$

and

$$\beta\tau = f_3(c, s_m), \quad (\text{V.3})$$

respectively ($f_1 \sim f_3$ are dimensionless functions of c and s_m). In order to investigate how the dynamic shear moduli depend on the temperature and the polymer volume fraction, let us rewrite (V.1) \sim (V.3) as

$$\frac{v_0 G_\infty}{k_B T_0} = \frac{\phi}{N} \frac{T}{T_0} f_1(c(T/T_0, N, \phi), s_m), \quad (\text{V.4})$$

$$\frac{v_0 \beta_0 \eta_0}{k_B T_0} = \frac{\phi}{N} \frac{T}{T_0} e^{T_0/T-1} f_2(c(T/T_0, N, \phi), s_m), \quad (\text{V.5})$$

$$\beta_0 \tau = e^{T_0/T-1} f_3(c(T/T_0, N, \phi), s_m), \quad (\text{V.6})$$

respectively. We have put $W = \epsilon$ in the derivation of (V.5) and (V.6), In this case, the dissociation rate at temperature T is written as

$$\beta = \omega_0 e^{-\epsilon/k_B T} = \beta_0 e^{1-T_0/T} \quad (\text{V.7})$$

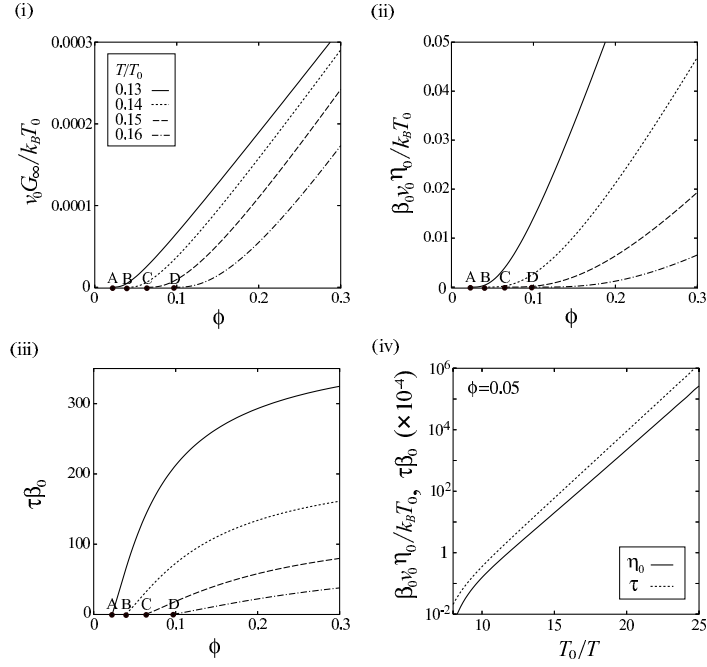


FIG. 9: (i) The plateau modulus, (ii) zero-shear viscosity, and (iii) relaxation time plotted against the polymer volume fraction for several temperature with $s_m = 20$, $N = 100$ and $\lambda_0 = 1$. Marked points A, B, C, D on the horizontal axis of (i) indicate the critical volume fraction ϕ^* for each temperature corresponding to the points in Fig.2 (b). (iv) Arrhenius plots of the zero-shear viscosity and the relaxation time with $\phi = 0.05$, $s_m = 20$, $N = 100$ and $\lambda_0 = 1$.

where β_0 is the dissociation rate at temperature T_0 . Recall that the reduced concentration depends on the temperature, molecular weight, and the polymer volume fraction as $c(T/T_0, N, \phi) = 2\phi\lambda_0 e^{T_0/T}/N$. Thus, for example, the zero-shear viscosity (V.5) depends on the temperature through β , c and a prefactor. The unitless plateau modulus (V.5), zero-shear viscosity (V.5) and relaxation time (V.6) are shown in Fig.9 (i) ~ (iii) as a function of the polymer volume fraction for several temperature. Volume fraction is varying across the sol/gel transition line drawn in Fig.2 (b) for each temperature. If the volume fraction ϕ is small, G_{∞} and η_0 depend on ϕ through the reduced concentration c and a prefactor, while they are approximately proportional to ϕ if ϕ (and hence c) is large because f_1 and f_2 depend only weakly on c (see Fig.7) in this case. On the other hand, τ depends on ϕ only through c . As shown in Fig.9 (iv), the zero-shear viscosity and the relaxation time approximately show the Arrhenius law temperature dependences. At higher temperature, we can see a slight deviation from the Arrhenius law. This deviation stems from the fact that η_0 and τ depend on T not only through β (see (V.7)) but also through c (and a prefactor in the case of η_0). On the other hand, η_0 and τ depend only weakly on c at lower temperature, and hence they show approximately the Arrhenius law. We can guess from (V.5) and (V.6) that the dynamic shear moduli at temperature T can be superimposed to the curve at the reference temperature T_{ref} if they are horizontally and vertically shifted by a factor of a_T and b_T , respectively, where

$$a_T = \exp \left[-T_0 \left(\frac{1}{T_{ref}} - \frac{1}{T} \right) \right] \cdot \frac{f_3(c(T/T_0, N, \phi), s_m)}{f_3(c(T_{ref}/T_0, N, \phi), s_m)}, \quad (\text{V.8a})$$

$$b_T = \frac{T_{ref}}{T} \cdot \frac{f_1(c(T_{ref}/T_0, N, \phi), s_m)}{f_1(c(T/T_0, N, \phi), s_m)}. \quad (\text{V.8b})$$

Especially for larger ϕ or lower T , (V.8) is approximately written as

$$a_T \simeq \exp \left[-T_0 \left(\frac{1}{T_{ref}} - \frac{1}{T} \right) \right], \quad (\text{V.9a})$$

$$b_T \simeq \frac{T_{ref}}{T} \quad (\text{V.9b})$$

It has been revealed by Annable *et al.* that the shift factor given by (V.9) produces the master curve successfully.[2]

In Fig.10 (i), we compare theoretically predicted dynamic shear moduli (i.e., plateau modulus, zero-shear viscosity and relaxation time) with experimental observation for aqueous solutions of telechelic PEO of 20 kg/mol [11] and 35

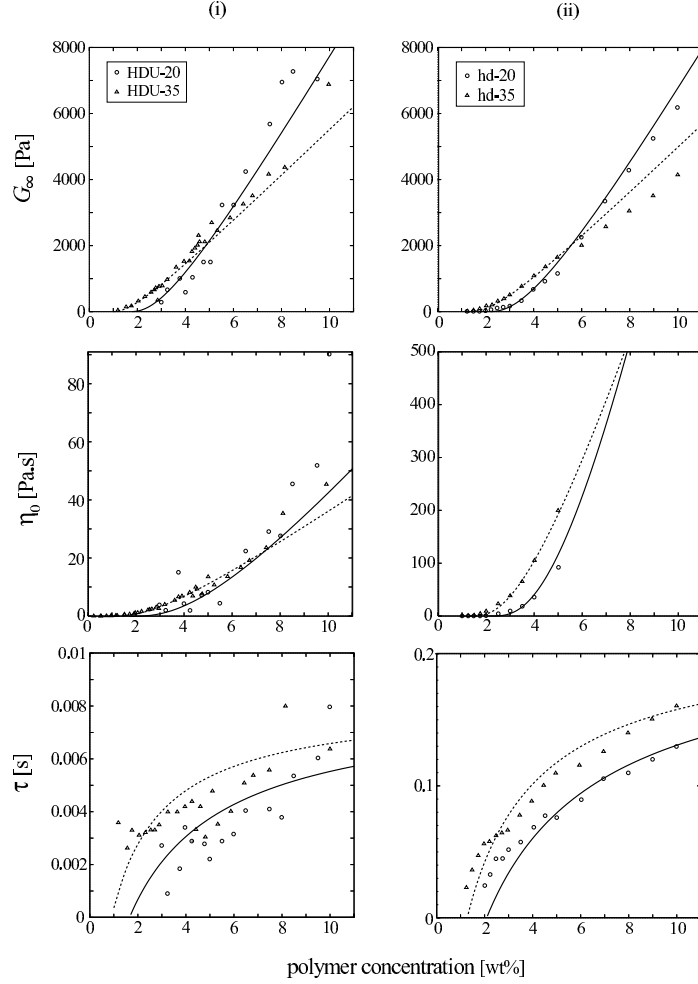


FIG. 10: Comparison between the theoretically obtained plateau modulus (top), zero-shear viscosity (middle), relaxation time (bottom) for the saturating junction model (lines) and experimental data obtained for (i) telechelic PEO with narrow molecular weight distribution and fully end-capped with C_{16} alkanes ($M_w=20,000$ for HDU-20 [11] and $M_w=35,000$ for HDU-35 [7]) and (ii) HEUR end-capped with the same alkanes ($M_w=20,000$ for hd-20 and $M_w=33,100$ for hd-35 [2]). Values of molecular parameters s_m , β and λv_0 used to draw theoretical curves are listed in TABLE I.

kg/mol [7] with narrow-molecular-weight distribution and fully end-capped with C_{16} alkanes. We call these polymers HDU-20(35) according to ref..[11] The reduced concentration c was converted into the polymer concentration in weight percentage c_w through a relation $c = (2000N_A/M)\lambda v_0 c_w$ (N_A is Avogadro's number). We have three molecular parameters for a given molecular weight: s_m , λv_0 and β . (Note that β is not required to calculate G_∞ .) Values of these parameters used to draw theoretical curves are listed in TABLE I. We find better agreements between theory and experiment than in the case that the short lifetime of superbridges is not taken into consideration.[12] The value of λv_0 increases with increasing the molecular weight. This indicates that the effective volume v_0 of a functional group increases with increasing the chain length. In Fig.10 (ii), we attempt to fit theoretical curves to experimental data reported by Annable *et al.* [2] for HEUR of the similar molecular weight (but with broader molecular weight distribution) and end-capped with C_{16} alkanes. They are called hd-20(35) after ref..[11] Parameter values adopted to fit experimental data are also listed in TABLE I. We still find a good agreement between theory and experiment in spite of a broader molecular weight distribution of hd polymers. A difference in the value of λv_0 between HDU and hd for each (averaged) molecular weight might stem from a difference in the polydispersity of the PEO backbone. A ratio between the value of λv_0 for HDU-20 and for HDU-35 (3.2) is close to that between hd-20 and hd-35 (2.9). A discrepancy in the value of β for HDU and for hd might stem from the difference in the coupling agents between the alkanes and the PEO backbone as suggested in refs..[7, 11]

polymer	s_m	β [1/s]	$\lambda v_0 \times 10^{23}$ [m ³]
HDU-20	20	60	0.1
HDU-35	20	60	0.32
hd-20	20	2.3	0.08
hd-35	20	2.3	0.23

TABLE I: Values of molecular parameters used in Fig.10.

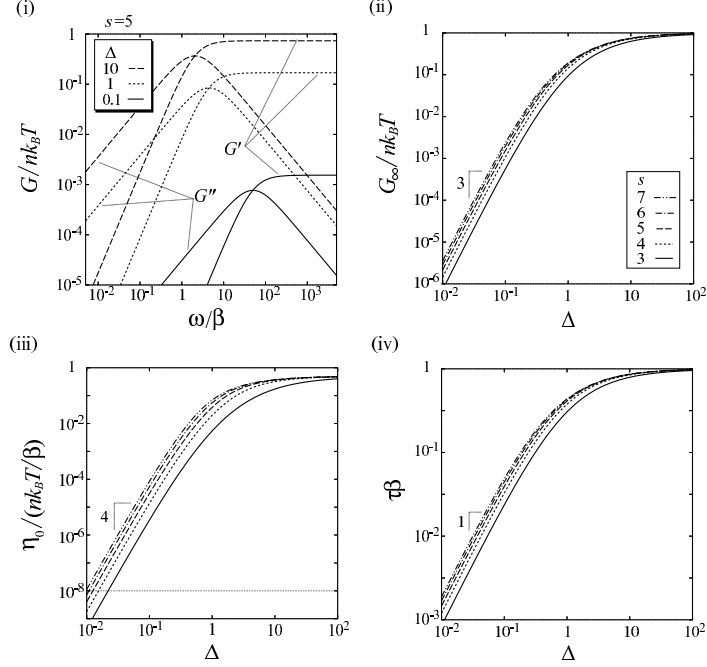


FIG. 11: (i) The dynamic shear moduli (reduced by $nk_B T$) obtained for the fixed multiplicity model as a function of the frequency. The relative concentration deviation is varying from curve to curve, while the multiplicity of the junction is fixed at $s = 5$. (ii) The reduced plateau modulus, (iii) reduced zero-shear viscosity, and (iv) relaxation time plotted against the relative concentration deviation for several multiplicities.

B. Fixed Multiplicity Model

Fig.11 shows the dynamic shear moduli of the fixed multiplicity model together with the plateau modulus, zero-shear viscosity and relaxation time plotted against the relative concentration deviation. These quantities obey the same critical behavior as in the saturating junction model, i.e., they increase as $G_\infty \sim \Delta^3$, $\eta_0 \sim \Delta^4$ and $\tau \sim \Delta$ with increasing Δ near the sol/gel transition concentration.

In Fig.12, theoretical curves are compared with experimental data for telechelic PEO. Values of parameters used to draw theoretical curves are listed in TABLE II. We find a disagreement between theory and experiment in the relaxation time; theoretical curves increase more rapidly with increasing the concentration than experimental data, and they become approximately flat above a certain concentration. This is because the fraction of junctions with the path connectivity $i = 2$ (or, in other words, the number of superbridges) is small when the junction can take only a single multiplicity.^f This tendency becomes more pronounced with increasing the multiplicity because the fraction of $i = 2$ junctions is smaller for larger multiplicity. Thus we guess that the multiplicity should not be fixed at a single value. In real systems, junctions might be cores of flower-like micelles and the aggregation number (i.e., the number of chains per junction), say s_{flower} , is almost independent of the polymer concentration as some researchers

^f The relaxation time does not depend on the concentration for the fixed multiplicity model if effects of superbridges are not taken into account.[12]

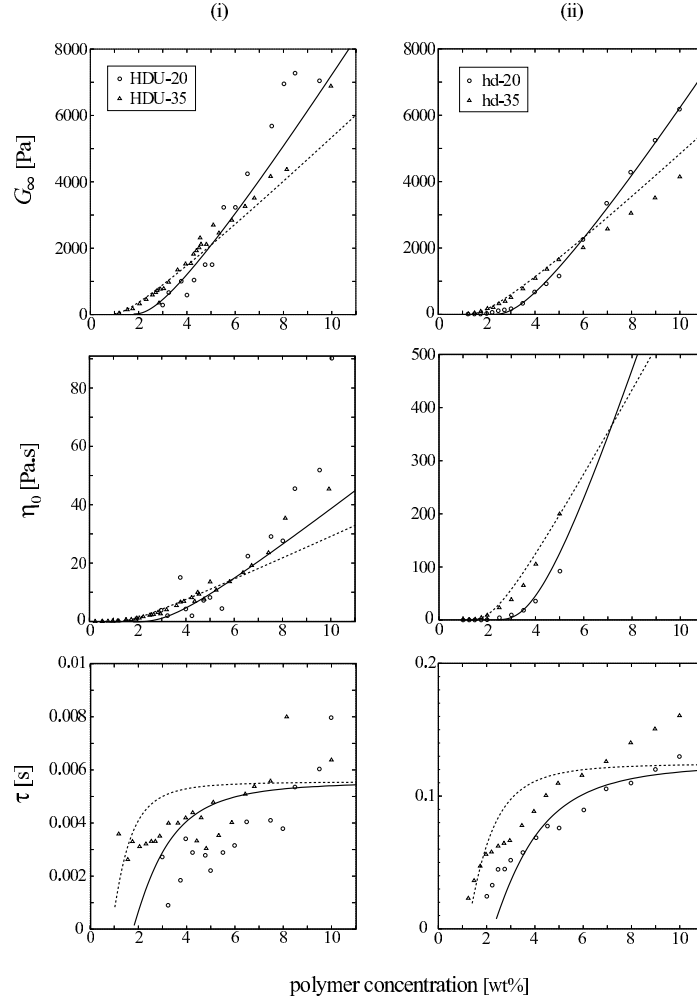


FIG. 12: Comparison between the theoretically predicted plateau modulus (top), zero-shear viscosity (middle), relaxation time (bottom) for the fixed multiplicity model (lines) and experimental data observed for (i) telechelic PEO with narrow molecular weight distribution fully end-capped with C_{16} alkanes ($M_w=20,000$ for HDU-20 [11] and $M_w=35,000$ for HDU-35 [7]) and (ii) HEUR end-capped with the same alkanes ($M_w=20,000$ for hd-20 and $M_w=33,100$ for hd-35 [2]). Values of molecular parameters s , β and λv_0 used to draw theoretical curves are listed in TABLE II.

polymer	s	β [1/s]	$\lambda v_0 \times 10^{23}$ [m ³]
HDU-20	6	90	0.09
HDU-35	6	90	0.32
hd-20	6	4	0.07
hd-35	6	4	0.23

TABLE II: Parameter values used in Fig.12.

indicated. In this case, the number of bridge and dangling chains emerged from the junction (i.e., multiplicity of the present theory) can be less than s_{flower} . This situation corresponds to the saturating junction model, not the fixed multiplicity model. This might be the reason why the saturating junction model can describe the dynamic shear moduli of telechelic PEO better than the fixed multiplicity model.

VI. SUMMARY

We developed the theory of transient networks with junctions of limited multiplicity. The global information was incorporated into the theory by introducing the elastically effective chains (active chains) according to the criterion by Scanlan and Case and by considering the effect of superbridges whose backbone is formed by several chains connected in series. Linear viscoelasticities of the network were studied as functions of thermodynamic quantities. Near the critical concentration for the sol/gel transition, superbridges are infinitely long along the backbone and their number is comparable with that of primary bridges. Thus the mean lifetime of bridges is quite short near the critical point and so does the relaxation time. It was found that the relaxation time is proportional to the concentration deviation Δ near the sol/gel transition concentration. Since the plateau modulus increases as the cube of Δ as a result of the mean-field treatment, the zero-shear viscosity increases as Δ^4 near the gelation point. Obtained dynamic shear moduli as a function of the polymer concentration were found to agree well with the experimental data observed for aqueous solutions of telechelic poly(ethylene oxide).

We assumed in this theoretical model that intramolecular associations generating looped chains are absent. Looped chains are supposed to compete with intermolecular association that causes bridge chains at a junction due to the limitation of the multiplicity that the junction can take. Such competition might influence the viscoelasticity of the system. This effect as well as the influence of additives such as surfactant or single end-capped polymers will be studied in the forthcoming paper.

-
- [1] M. A. Winnik, and A. Yekta, **2**, 424 (1997).
 - [2] T. Annable, R. Buscall, R. Ettelaie, and D. Whittlestone, *J. Rheol.*, **37**, 695 (1993).
 - [3] R. D. Jenkins, D. R. Bassett, C. A. Silebi, and M. S. El-Aasser, *J. Appl. Polym. Sci.*, **58**, 209 (1995).
 - [4] A. Yekta, B. Xu, J. Duhamel, H. Adiwidjaja, M. A. Winnik, *Macromolecules*, **28**, 956 (1995).
 - [5] E. Alami, M. Almgren, W. Brown, and J. François, *Macromolecules*, **29**, 2229 (1996).
 - [6] Q. T. Pham, W. B. Russel, J. C. Thibeault, and W. Lau, *Macromolecules*, **32**, 2996 (1999).
 - [7] Q. T. Pham, W. B. Russel, J. C. Thibeault, and W. Lau, *Macromolecules*, **32**, 5139 (1999).
 - [8] Y. Séréro, V. Jacobsen, J. -F. Berret, and R. May, *Macromolecules* **33**, 1841 (2000).
 - [9] D. Calvet, A. Collet, M. Viguier, J. -F. Berret, and Y. Séréro, *Macromolecules*, **36**, 449 (2003).
 - [10] P. Kujawa, H. Watanabe, F. Tanaka, F. M. Winnik, *Eur. Phys. J. E*, **17**, 129 (2005).
 - [11] X. -X. Meng, W. B. Russel, *J. Rheol.*, **50**, 189 (2006).
 - [12] T. Indei, submitted for publication (2006).
 - [13] J. Scanlan, *J. Polym. Sci.*, **43**, 501 (1960).
 - [14] L. C. Case, *J. Polym. Sci.*, **45**, 397 (1960).
 - [15] F. Tanaka, and W. H. Stockmayer, *Macromolecules*, **27**, 3943 (1994).
 - [16] F. Tanaka, and M. Ishida, *Macromolecules*, **29**, 7571 (1996).
 - [17] D. S. Pearson, and W. W. Graessley, *Macromolecules*, **11**, 528 (1978).
 - [18] P. J. Flory, *Principles of Polymer Chemistry*, Cornell University Press: Ithaca, NY, 1953; Chapter 9.
 - [19] W. H. Stockmayer, *J. Chem. Phys.*, **11**, 45 (1943); *Ibid.* **12**, 125 (1944).
 - [20] F. Tanaka, and S. F. Edwards, *Macromolecules*, **25**, 1516 (1992).
 - [21] F. Tanaka, and S. F. Edwards, *J. Non-Newtonian Fluid Mech.*, **43**, 247, 273, 289 (1992).
 - [22] T. Indei, F. Tanaka, *J. Rheol.*, **48**, 641 (2004).
 - [23] K. Fukui, and T. Yamabe, *Bull. Chem. Soc. Jpn.*, **40**, 2052 (1967).
 - [24] M. Rubinstein, and A. N. Semenov, *Macromolecules*, **31**, 1386 (1998).